



3D Virus Imaging at XFEL.

Simulation of Coherent X-ray Diffraction and Data Processing

Starykh Elizaveta

Moscow Institute of physics and technology, Dolgoprudny, Russia

Supervisors: Max Rose, Ivan Vartanians
DESY, Hamburg, Germany

Keywords:

single particle imaging, x-ray free electron laser, Rice Dwarf virus.

Abstract

In many fields of science the ability to visualize the three dimensional organization of component parts is proving crucial to our understanding of the mechanisms involved in atomic and molecular processes. This is occurring in fields as diverse as whole-cell imaging in biology, the study of the minimum energy pathway for crack propagation in brittle solids, and the internal structure of the new labyrinthine mesoporous structures developed by inorganic chemists for a wide range of applications. The field of coherent x-ray diffraction imaging (also known as diffraction microscopy) is expected to make a significant contribution to this effort. In this method an image is reconstructed from measurements of the far-field scattered intensity of an isolated and nonperiodic object. First single particle imaging (SPI) experiments performed at the Linac Coherent Light Source (LCLS) have been very successful, producing single-shot coherent diffraction images of viruses, bacteriophages, organelles, and cyanobacteria to name a few. A variety of other biological structures have been imaged with the goal of creating data sets for algorithm development. First steps have been taken to assemble single shot images into three dimensional data sets. In addition to biological systems, single shot diffractive imaging has been used to study the morphology of aerosols, power density dependent damage processes in atomic clusters, and superfluid quantum systems.

Contents

1. Introduction	3
2. Theory of the experiment.....	Error! Bookmark not defined. 4 Error! Bookmark not defined.
3. SPI experiment stages	6
4. Simulation parameters.....	8
5. Simulation results (3D reconstructed virus, optimization)	Error! Bookmark not defined. 9
6. Reconstruction	11
7. Conclusion	12
8. Acknowledgements.....	Error! Bookmark not defined. 13
References	Error! Bookmark not defined.
Appendix	Error! Bookmark not defined.

1. Introduction

Single particle imaging (SPI) is a method of imaging isolated particles, molecules and viruses at resolutions limited, in principle, by only the wavelength and largest scattering angles recorded. There are advantages of using SPI, such as:

- Wide application on non-crystallic structures, for example on proteins and viruses
- It is possible to create a short pulse, powerful enough to obtain needed information before the object's destruction

That is why single particle imaging becomes high-demand. In this work we simulate the experiment of SPI, using Rice Dwarf Virus (RDV) as an object. A single virus is irradiated with X-rays. Although this irradiation destroys the sample due to development of free electron laser (see [LINK]), it is possible to create a pulse short and powerful enough to obtain needed information before the destruction. This method is called "Diffract and destroy". The resolution of this form of microscopy is limited by the wavelength, the amount of pixels on the detector and largest scattering angles recorded.

2. Theory of the experiment

The incident x-ray wave field interacts with a 3D periodic or nonperiodic object through the scattering potential of the object, $o(\mathbf{x}) = r_e \rho(\mathbf{x})$, where $\rho(\mathbf{x})$ is the complex electron density and r_e is the classical electron radius. This object scattering function may be decomposed into a Fourier representation of 3D spatial frequencies \mathbf{u} , with complex amplitudes

$$O(\mathbf{u}) = F\{o(\mathbf{x})\} \equiv \int o(\mathbf{x}) \exp(2\pi i \mathbf{u} \cdot \mathbf{x}) d\mathbf{x},$$

in which each spatial frequency can be thought of as a volume grating. In the case of coherent diffraction imaging a plane wave with wave vector \mathbf{k}_{in} is incident on the object, and the intensity of the scattered field in the direction of the wave vector \mathbf{k}_{out} is measured on a 2D pixellated detector in the diffraction far field. This detector is typically centered on the forward direction but in principle could be oriented in any angle to the incident beam (see Fig. 1). For elastic scattering, only the volume gratings that satisfy Bragg's law will scatter, and the wave-vector transfer $\mathbf{q} = \mathbf{k}_{out} - \mathbf{k}_{in}$ will be equal to the grating spatial frequency; that is, $\mathbf{q} = \mathbf{u}$. Since the magnitudes $|\mathbf{k}_{out}|$ and $|\mathbf{k}_{in}|$ are constant and equal to $1/\lambda$, these spatial frequencies \mathbf{u} lie on the Ewald sphere of radius $1/\lambda$, where λ is the x-ray wavelength.

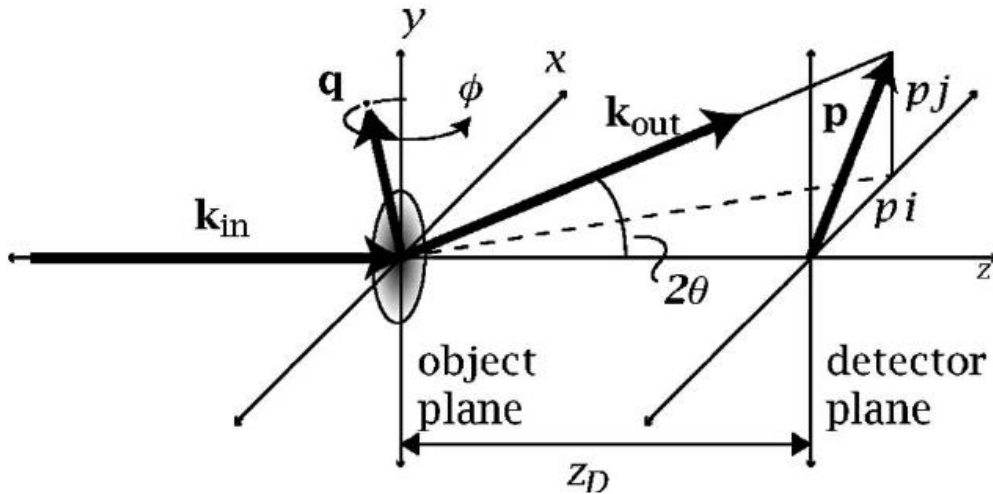


Figure 1. Scattering geometry for coherent x-ray diffraction imaging. The sample is rotated about the y axis by an angle ϕ .

This construction is equivalent to the condition that to scatter light by an angle 2θ from the forward direction (the z axis), the volume grating must be tilted by an angle θ from perpendicular to the forward direction (Bragg's law).

With the convention used here we have $|\mathbf{q}| = q = (2/\lambda)\sin\theta$. The diffraction amplitudes in the direction \mathbf{k}_{out} are proportional to $O(\mathbf{q})$, and in diffraction imaging we measure the intensities, proportional to $|O(\mathbf{q})|^2$. In particular, in the Born approximation (which can be thought of in this context as single scattering), the number of photons per second measured in a CCD pixel, with solid angle Ω , is given by

$$I(\mathbf{q}; \Omega) = I_0 \Omega P |O(\mathbf{q})|^2,$$

where I_0 is the flux (photons per second per unit area) of the incident plane wave on the sample and P is the polarization factor; $P = (1 + \cos^2\psi)/2$ for unpolarized light, with $\psi = 2\theta$.

The complex scattering potential $o(\mathbf{x})$ that we aim to recover from measurements of $I(\mathbf{q})$ is related to the complex refractive index $n(\mathbf{x})$ of the object by

$$o(\mathbf{x}) = r_e \rho(\mathbf{x}) = \frac{\pi}{\lambda^2} [1 - n^2(\mathbf{x})].$$

In the soft x-ray region the complex refractive index is usually written in terms of the optical constants as $n = 1 - \delta(\mathbf{x}) - i\beta(\mathbf{x})$. For optical constants much less than unity, which is generally the case for soft x rays, previous equation can then be well approximated by

$$o(\mathbf{x}) \approx \frac{2\pi}{\lambda^2} [\delta(\mathbf{x}) - i\beta(\mathbf{x})] = \frac{2\pi}{\lambda^2} \Delta n(\mathbf{x}).$$

3. SPI experiment stages

Here we will briefly describe the stages of our simulations.

In the simulation we obtain the atomic structure of Rice Dwarf Virus from the Protein Data Bank (see [6]). Then we simulate diffraction patterns of this structure using MOLTRANS program kindly provided by Edgar Weckert. It is worth mentioning that we already know orientations of this diffraction patterns, that is why we do not have to use co-called “Expansion-Maximization-Compression” algorithm.

See Figures 2, 3 and 4.

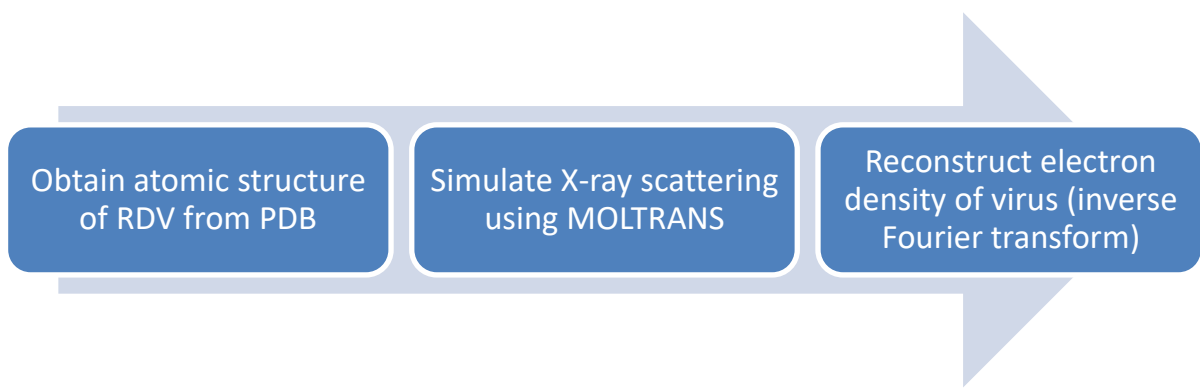


Figure 2. A schematic description of the process

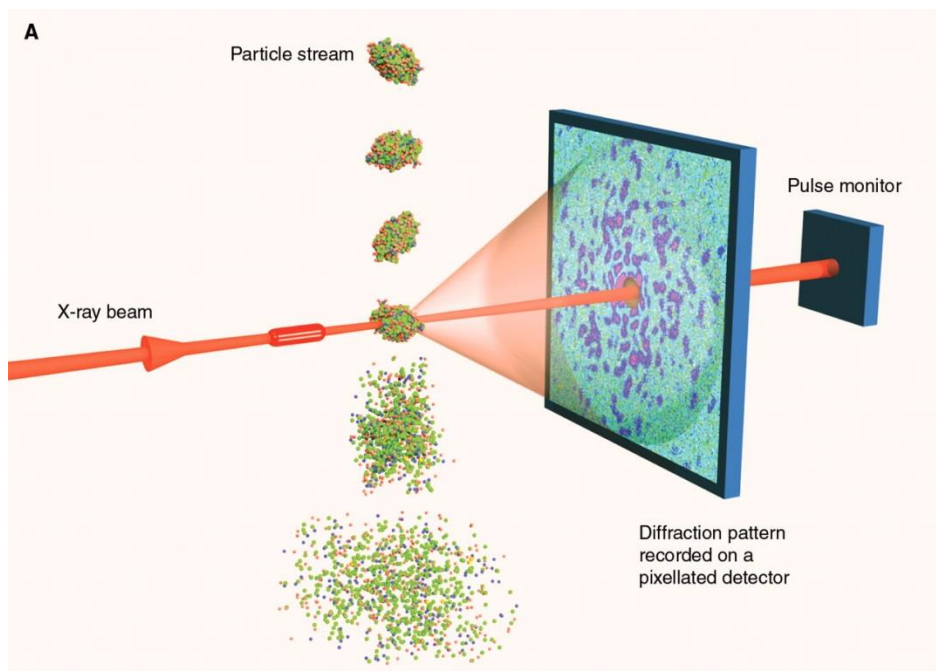


Figure 3. Experimental setup

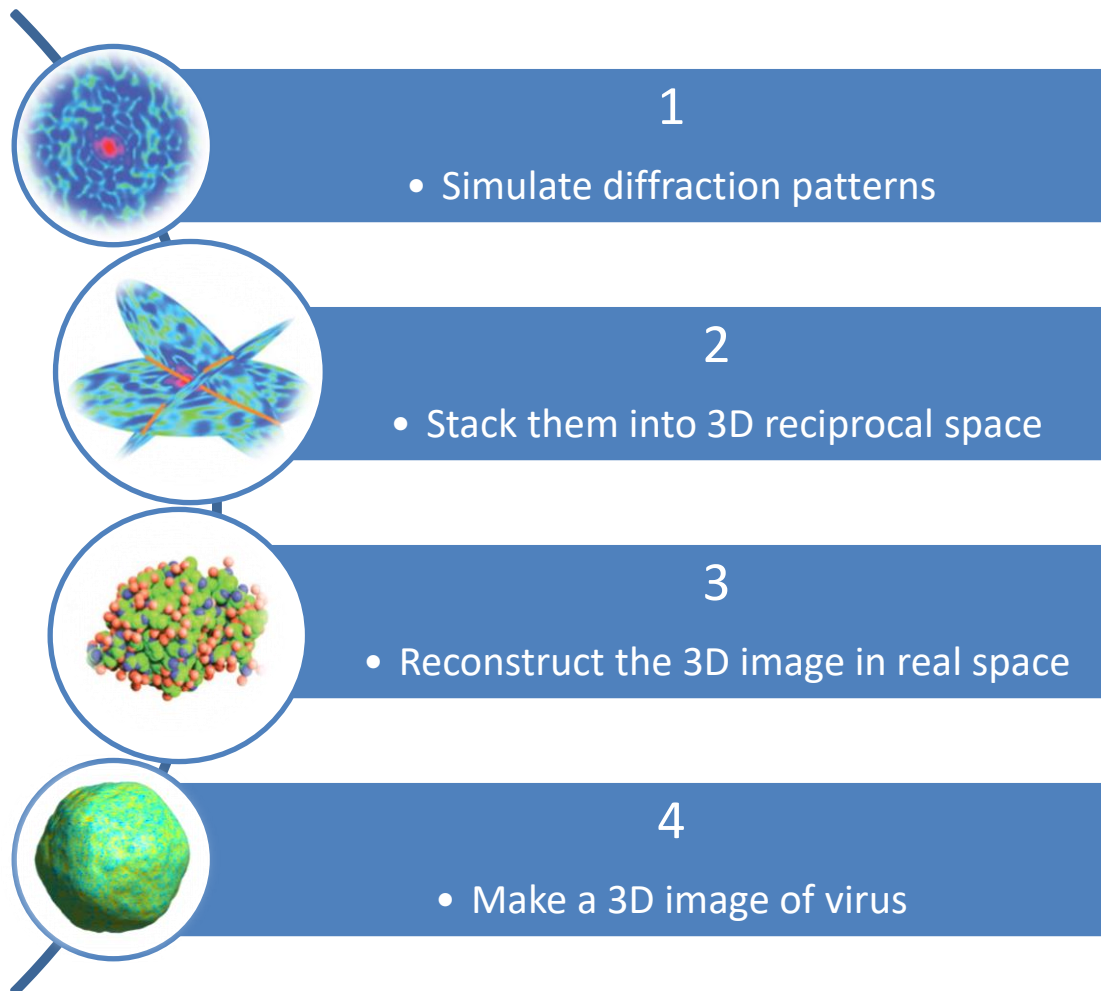


Figure 4. Simulation stages

4. Simulation parameters

In our simulation we used the following set of parameters:

Distance from the virus to the detector	300 mm
The side length of the square plane detector	265.5 mm
The wavelength	1.77 \AA
The number of pixels on the detector	1024×1024
Fluence	$10^2 - 10^4$
Number of diffraction patterns	25000
Beam focus:	$2 \text{ }\mu\text{m}$

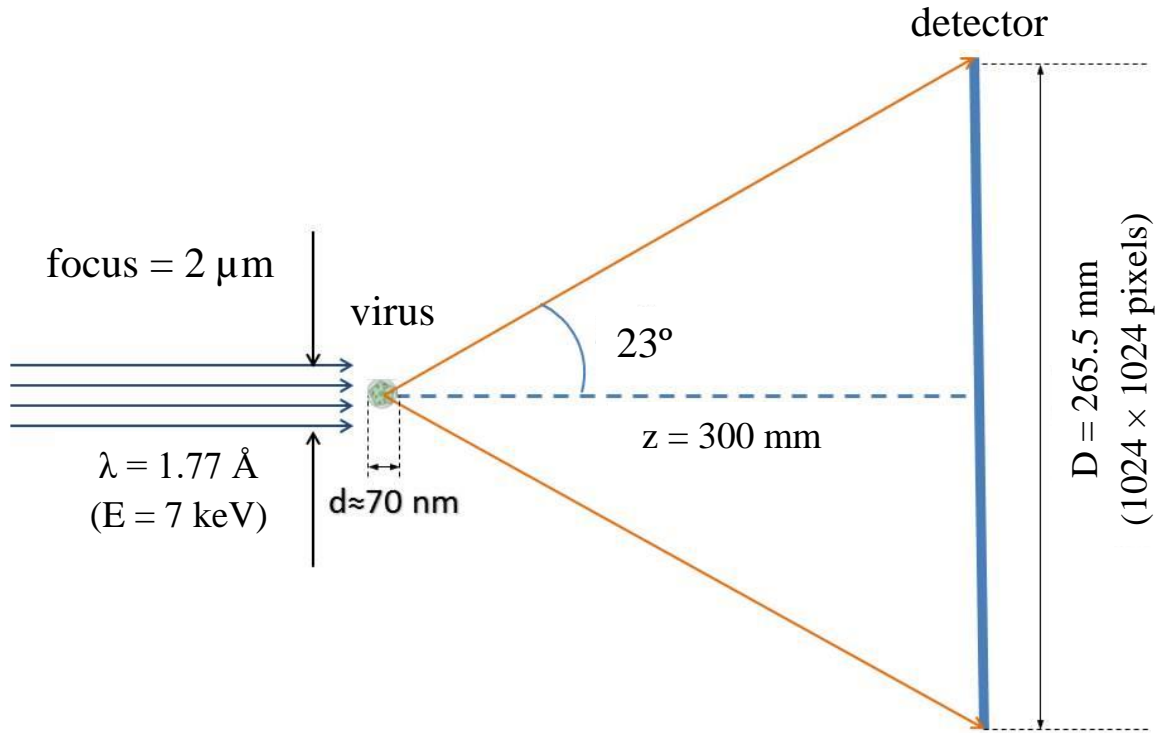


Figure 5. Experimental setup and simulation parameters

5. Simulation results

The number of diffraction patterns is expected to affect the resolution and also the reconstruction reliability. It is ambiguous questions how to estimate the resolution limit from the PSD plot. Since the standard deviation of Poisson noise is equal to the square root of the average number of events N , the signal-to-noise ratio (SNR) is given by

$$SNR = \frac{N}{\sqrt{N}} = \sqrt{N}.$$

There are some possibilities how we can look at the resolution limits.

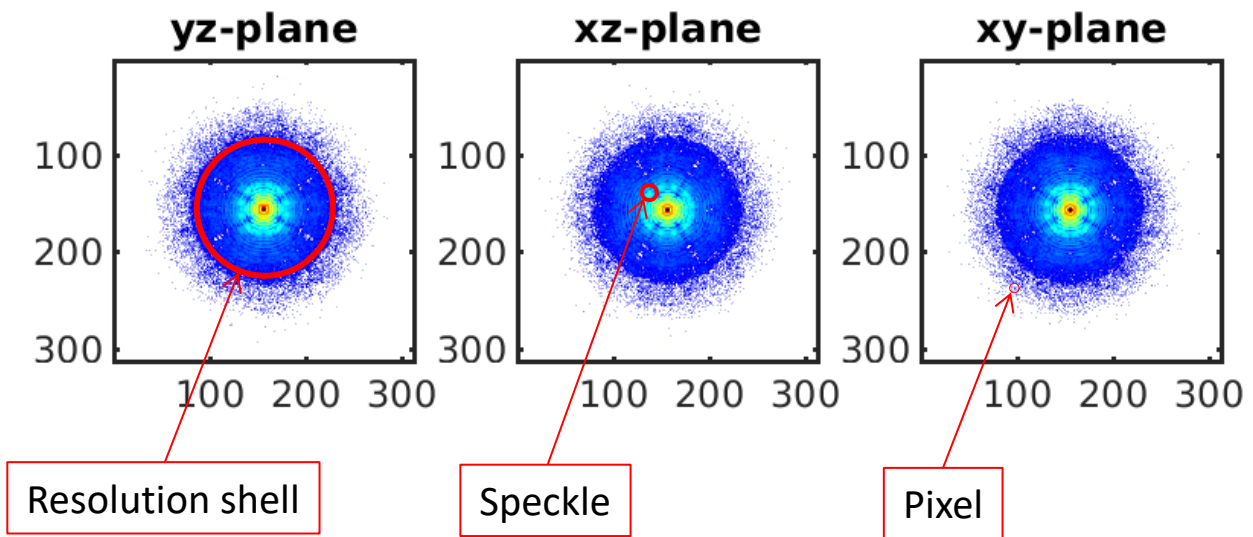


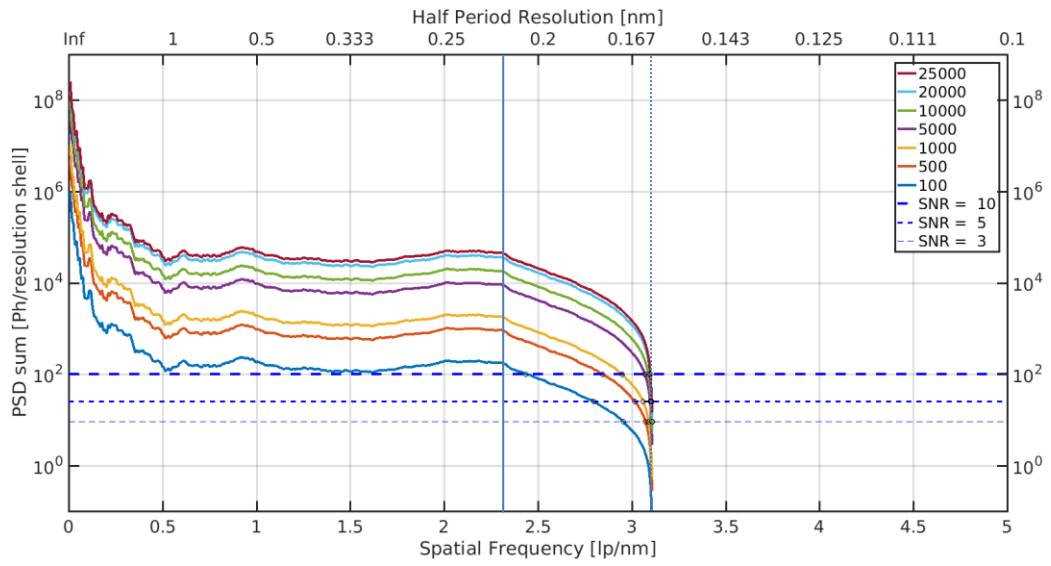
Figure 6. Explanation of terms which we used to talk about resolution

The PSD plots calculated from the reciprocal space are shown below.

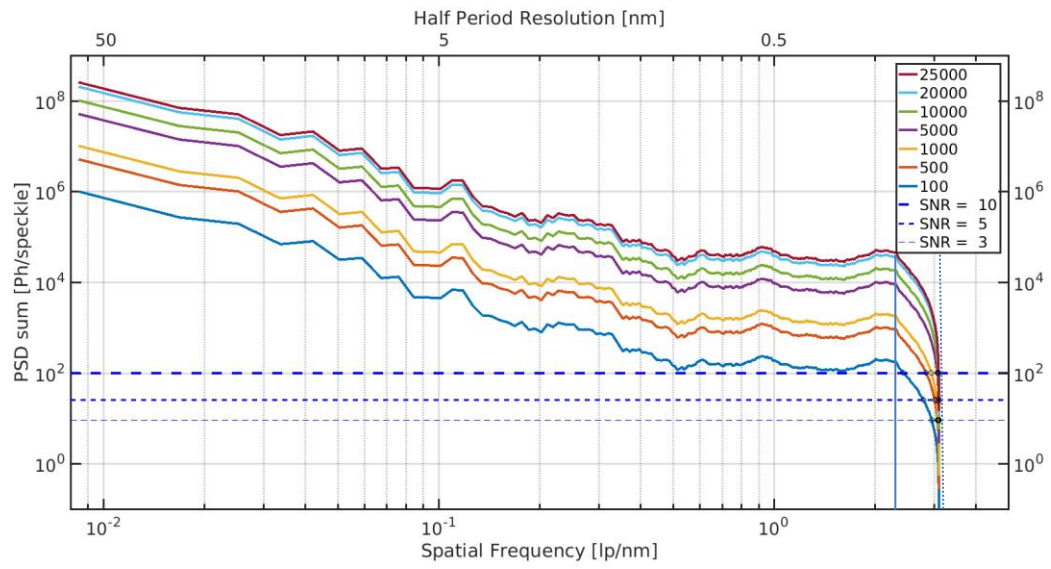
- a) In case of resolution shell (see Figure 7.a)
- b) In case of speckle (see Figure 7.b)
- c) In case of pixel (see Figure 7.c)

Using this PSD plots we can figure out how many diffraction patterns do we need to reach certain resolution. For that purpose we can find the intersections with thresholds which defined Signal-to-Noise-Ratios (SNR) equal to 3, 5 and 10. Each intersection lead us to the value of Half Period Resolution (see Figure 7).

a)



b)



c)

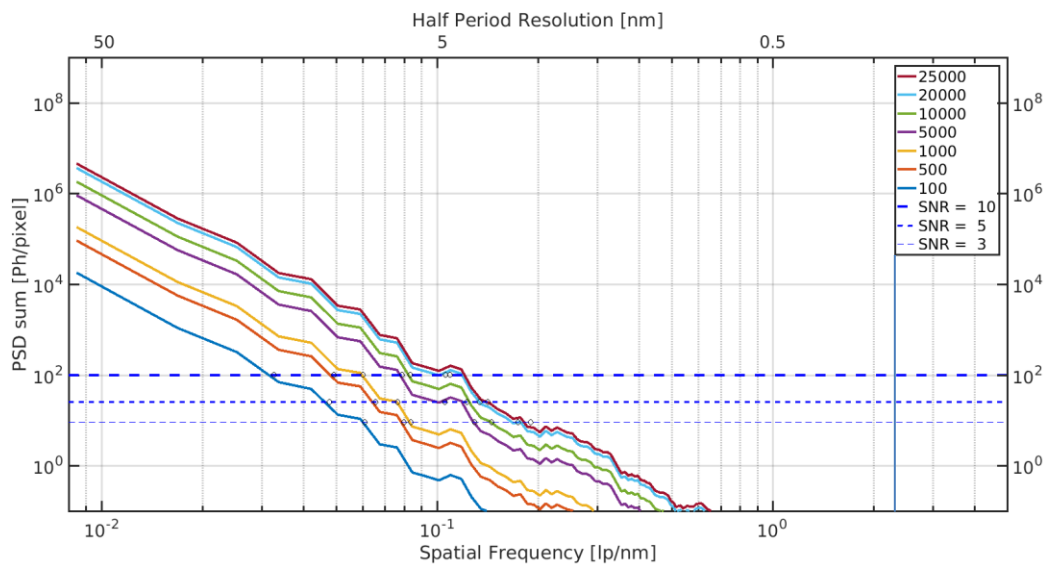


Figure 7. PSD plots and intersections with the SNR thresholds

6. Reconstruction

At the next stage of reconstruction algorithm took place and the result is shown in Figure 8.

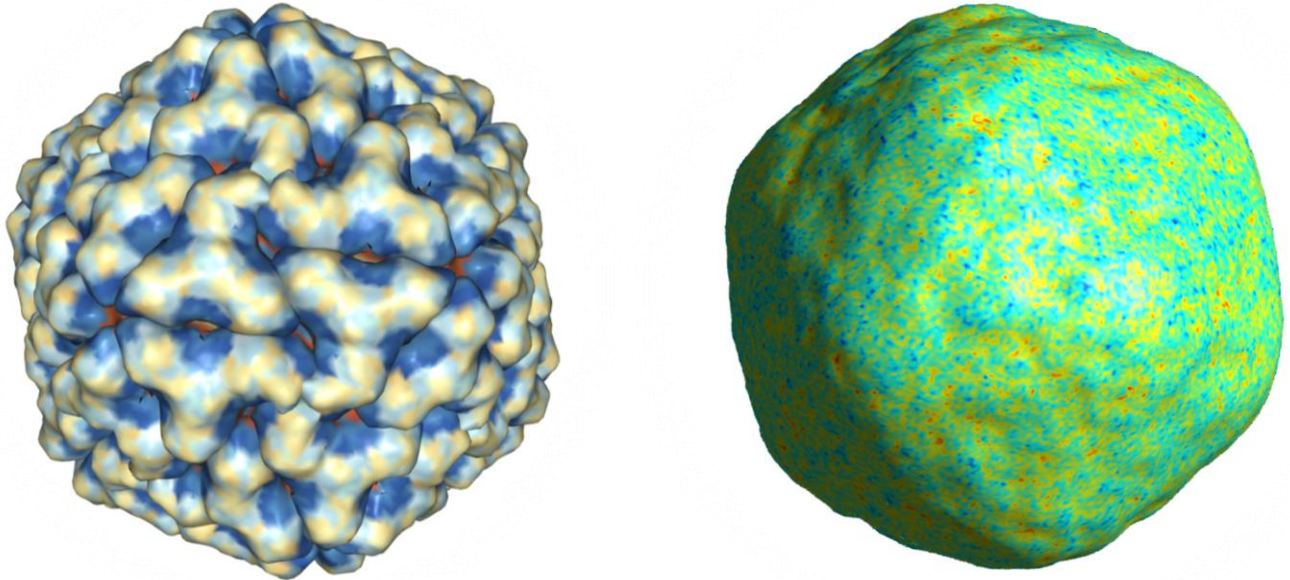


Figure 8. Comparison of RDV surface: a) image obtained from PDB, b) reconstructed image

Now we can compare it with the surface image taken from Protein Data Bank (see [6]). As we can see the reconstructed virus has the same shape and icosahedral symmetry.

7. Conclusion

We demonstrated x-ray diffraction imaging with high resolution in all three dimensions, as determined by a quantitative analysis of the reconstructed volume images. These images are retrieved from the three-dimensional diffraction data using no a priori knowledge about the shape or composition of the object, which has never before been demonstrated on a nonperiodic object. We also construct two-dimensional images of thick objects with greatly increased depth of focus (without loss of transverse spatial resolution). These methods can be used to image biological and materials science samples at high resolution with x-ray undulator radiation and establishes the techniques to be used in atomic-resolution ultrafast imaging at x-ray free-electron laser sources.

What have been done:

- Simulated 25,000 diffraction patterns
- Stacked them into 3D reciprocal space
- Used pre-allocation to reduce processing time
- Reconstructed the RDV surface from our simulations

8. Acknowledgements

I would like to acknowledge Max Rose and Ivan Vartanians for their intense support and help during whole summer program. I would also like to thank Max Rose, Nastasia Mukharamova, Luca Gelisio, Oleg Gorobtsov, Young Yong Kim, Ruslan Khubbutdinov, Sergey Lazarev and Ivan Vartanians for beneficial and fruitful discussions and assistance.

I also thank Edgar Weckert for providing me with MOLTRANS program and consulting on it. Additionally, I would like to thank Olaf Behnke, Rainer Gehrke and all DESY Summer Student Program 2017 Organizing Team for the opportunity to participate in this fantastic program.

References

- [1] Anna Munke, Jacob Andreasson, Andrew Aquila, Salah Awel, Kartik Ayyer, Anton Barty, Richard J. Bean, et al. *Data Descriptor: Coherent diffraction of single Rice Dwarf virus particles using hard X-rays at the Linac Coherent Light Source*.
<https://www.nature.com/articles/sdata201664>.
- [2] M. Rose, S. Bobkov, D. Dzhigaev, K. Ayyer, A. Morgen, O. M. Yefanov, R. P. Kurta, A. Khudorozhkov, C. H. Yoon, A. Aquila, A. Barty and I. A. Vartanyants. *Single Particle Imaging: PR772 virus reconstruction from X-ray free electron laser diffraction intensities*.
- [3] Andreas Schropp and Christian G Schroer. *New Journal of Physics. Dose requirements for resolving a given feature in an object by coherent x-ray diffraction imaging*.
- [4] Henry N. Chapman, Anton Barty, Stefano Marchesini, Alexandr Noy, et al. *High-resolution ab initio three-dimensional x-ray diffraction microscopy*.
- [5] S. A. Bobkov, A. B. Teslyuk, R. P. Kurta, O. Yu. Gorobtsov, O. M. Yefanov, V. A. Ilyin, R. A. Senin and I. A. Vartanyants. *Sorting algorithms for single-particle imaging experiments at X-ray free-electron lasers*.
- [6] Protein Data Bank. Atomic structure of Rice Dwarf Virus.
<https://www.rcsb.org/pdb/explore/explore.do?structureId=1UF2>

Appendix A.

